THE JOURNAL OF PHYSICAL CHEMISTRY C

Article

Cite This: J. Phys. Chem. C 2019, 123, 23511−23519

pubs.acs.org/JPCC

Metal Chelating Polymer Thin Films by Surface-Initiated ROMP and Modification

Xuanli Deng, Liudmyla Prozorovska, and G. Kane Jennings*

Department of Chemical and Biomolecular Engineering, Vanderbilt University, Nashville, Tennessee 37235, United States

Supporting Information

ABSTRACT: We report the surface-initiated ring-opening metathesis polymerization (SiROMP) of hydroxamic acid-containing, metal-chelating polymer thin films. SiROMP of *trans*-5-norbornene-2,3-dicarbonyl chloride (NBDAC) is introduced as a versatile platform to achieve many functional polymer films via simple exposure of pNBDAC films to reagents. This modification strategy owes its success to the fast and high-yield reaction of acyl chlorides with alcohols, amines, water, and other molecules. The polymerization of NBDAC is performed with monomer in the vapor phase and exhibits rapid kinetics, producing ∼400 nm thick films within 5 min. Because of the high reactivity of the acyl chloride groups in the film, the pNBDAC films are easily modified to produce side chains of carboxylic acids, esters, and amides via the reaction of the acyl group with water, alcohols, and amines, respectively. Exposure of the pNBDAC film to hydroxylamine results in a film with hydroxamic acid functionality that is capable of chelating various metal ions. The chelation process effectively cross-links the polymer chains to greatly improve the thermal and pH stability of the film in solution, elevate resistance against water and ion transfer, and alter the mechanical properties to a more solid-like film.

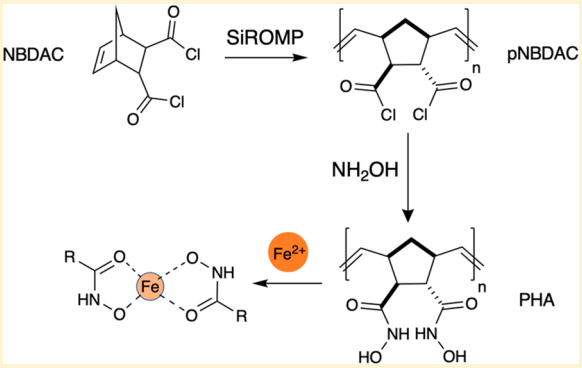

INTRODUCTION

Among the many techniques of polymer film preparation, surface-initiated polymerization (SIP) provides improved performance in constructing stable, controllable, and tunable polymer films with thicknesses from a few to a few thousand nanometers.[1−4] In SIP, the initiators are chemically coupled to the surface, often via the spontaneous chemisorption of a self-assembled monolayer (SAM), so that the polymerization happens directly from the surface. The chemical interactions between the polymer film and the surface contribute to the enhanced robustness of the film as a coating. Polymer coatings can be formed onto surfaces of nearly any geometric shape by using SIP,[2,3,5] and various well-developed polymerization methods can be utilized within SIP, which enables high control over film synthesis on the surface. In addition, unreacted molecules and byproducts are simply rinsed away from the bound film to simplify separations.

Many researchers have investigated the preparation of functional polymer films by SIP with different polymerization methods.[6−10] Among those methods, surface-initiated versions of atom-transfer radical polymerization (SiATRP) and ring-opening metathesis polymerization (SiROMP) are two that provide high control over the polymerization process, generally under mild and nonstringent conditions. ATRP has been well established and utilized in many research studies due to the control over film thickness and the tremendous variety of commercially available functional monomers that can undergo ATRP.[11,12] In contrast, ROMP has attracted less attention even though it exhibits significantly faster initiation and polymerization and enables the preparation of high molecular weight polymers with preservation of olefin functionality.[13−15]

There are several limitations in the SiROMP of monomers with functional groups. As a ring-opening process, ROMP is thermodynamically driven by release of the energy of ring strain, which establishes key requirements for the selection of ROMP monomers.[7,13,15] The most commonly used ROMP monomers are norbornene derivatives due to the high ring strain of the norbornene structure. However, not all norbornene-based monomers can be successfully polymerized from surfaces. The ease of the polymerization depends on the type of functional groups added to the norbornene structure due to either their reactivity with the catalyst or steric limitations. For example, norbornenecarboxylic acids have not been directly polymerized into polymer films through SiROMP in the literature, and thus, protection and deprotection processes have been required to obtain polymers with carboxylic acid groups via SiROMP.[16,17] Furthermore, some other groups of norbornene-based monomers, although they are suitable for SiROMP, are not commercially available. For these cases, time-consuming and costly monomer syntheses are required before SiROMP can yield polymer films with certain target compositions.[3,18] These requirements for and availability

Received: July 5, 2019
Revised: August 23, 2019
Published: September 4, 2019

DOI: 10.1021/acs.jpcc.9b06410
J. Phys. Chem. C 2019, 123, 23511−23519

of ROMP monomers have limited the development of functional polymers by this polymerization method.

Finding accessible new methods that can impart multiple functionalities to polymer films grown by SiROMP is critical. In this article, we report a method to prepare thin polymer films with various functionalities by employing Si-ROMP followed by simple modifications that are driven to completion. Acyl chloride groups are highly reactive toward water, alcohols, and amines at room temperature.[19] Therefore, the growth of polymer films with acyl chloride groups enables simple modification to introduce a wide range of versatile film compositions. A few researchers have synthesized acyl chloride-containing polymers in solution and esterified the reactive pendant groups to prepare functionalized polymers.[20−22] In fact, Hanson et al. reported polymerizations of *trans*-5-norbornene-2,3-dicarbonyl chloride (NBDAC) from both solution and nanoparticle surfaces,[23,24] and they utilized the obtained pNBDAC as scavengers or filters to facilitate separations of nucleophiles in organic reactions. They did not investigate pNBDAC as a thin film or as a platform to introduce functionality into polymer films. Beyond the limits of these investigations, polymer films with acyl chloride groups have not gained much attention and are not well established, despite their straightforward chemical modifications.

In this article, we report the preparation of pNBDAC thin films on smooth gold surfaces by SiROMP of the monomer from the vapor phase and the simple modification of pNBDAC to introduce many side-chain functionalities in polymer thin films. SIPs in vapor phase not only allow for a reduction of solvent consumption and a high purity of monomer but also reduce the occurrence of secondary metathesis reactions due to a reduced polymer chain mobility at the vapor/solid interface.[25,26] We prepare pNBDAC films on flat surfaces and use them as reactive intermediates to introduce various functionalities by simple acylation reactions to produce ester and amide linkages in high yield. We show that this modification method can routinely prepare many types of polymer films, all from a common base film of pNBDAC, with distinct functionalities to generate a wide range of film and surface properties. In this way, SiROMP of NBDAC and subsequent modification enable rapid access to many polymer film compositions that would be daunting and time-consuming to prepare by bulk polymer syntheses and associated separations. As a specific detailed example, we show that metal-chelating hydroxamic acid-containing polymer films can be obtained by simple modification of pNBDAC with hydroxylamine.

Metal chelating polymers attract great attention because of their important utilization in various areas, such as environmental protection,[27−31] medical therapy,[32−34] and analytical separations.[35,36] Among various chelating ligands, hydroxamic acid is one of the most widely utilized ligands as it is known to effectively chelate many different metal ions.[31,37−41] Polymers with hydroxamic acid functionality have been widely investigated in the past decades with most of the effort on bulk polymers and not thin films.[39−41] Thin films of hydroxamic acid functionality are useful to impart metal functionality to a variety of materials surfaces for applications as barrier films[27] and separations.[30] Tian et al. grafted poly(methyl acrylate) films onto a polypropylene surface and converted up to 30% of the methyl acrylates to hydroxamic acids for the chelation of iron from Fe^{3+} species.[27] In a separate study,[40] they were able to determine the pK_a of the surface grafted poly(hydroxamic acid) chains and investigate their coordination with Fe^{3+}.

Here, we show that a new type of polymer film composition containing hydroxamic side chains can be created in very high conversion by the reaction of pNBDAC with hydroxylamine. With this film, we demonstrate effective chelation of metals with high loadings, but our unique focus is on the physical properties imparted to the film by chelation. We use a combined approach of infrared spectroscopy, quartz crystal microbalance with dissipation, and electrochemical impedance spectroscopy to assess the effect of the chelated metals on thin film stability, mechanical properties, and ion transfer. The results reveal that these metal chelated films prepared by SiROMP are highly cross-linked and very robust.

EXPERIMENTAL SECTION

Materials. 4-Mercapto-1-butanol (95%), *trans*-3,6-endomethylene-1,2,3,6-tetrahydrophthaloyl chloride (NBDAC), Grubb's second-generation catalyst [$(H_2IMes)(PCy_3)(Cl)_2Ru{=}CHPh$], 3-bromopyridine, and 2 M ethylamine in THF were used as received from Sigma-Aldrich. Dichloromethane (DCM), pentane, 2-dimethylaminoethanol, aniline, hydroxylamine hydrochloride, iron(II) sulfate heptahydrate, copper(II) sulfate pentahydrate, cobalt(II) sulfate heptahydrate, zinc(II) chloride, iron(III) chloride, and ethanol (200 proof) were used as received from Fisher Scientific. Gold shot (99.99%) was obtained from J&J Materials, and chromium-coated tungsten rods were obtained from R.D. Mathis. Silicon (100) wafers were obtained from WRS Materials. QCM-D sensor crystals (quartz, 4.95 MHz, 14 mm diameter, polished, AT-cut with gold electrodes) were obtained from Biolin Scientific. Deionized water (10 MΩ) was purified by using a Millipore Elix filtration system.

Synthesis of $[(H_2IMes)(3\text{-Brpy})_2(Cl)_2Ru{=}CHPh]$. $[(H_2IMes)(3\text{-Brpy})_2(Cl)_2Ru{=}CHPh]$ (Grubbs catalyst third generation) was synthesized as described by Love et al.[18,42] Briefly, 3-bromopyridine (0.94 g, 5.9 mmol) and Grubbs second-generation catalyst (**2**) (0.5 g, 0.59 mmol) were added to a 20 mL vial with a screw cap. The reaction was stirred for 5 min with a color change from red to bright green. Pentane (20 mL) was added into the vial with the precipitation of a green solid. The vial was capped under air and placed in the freezer overnight. The green precipitate was vacuum filtered, washed with pentane (4 × 10 mL), and dried under vacuum to yield the title compound as a green powder.

Preparation of Gold Substrates. Silicon (100) wafers were rinsed with deionized water and ethanol and then dried in a nitrogen stream. Chromium (100 Å) and gold (1250 Å) were evaporated onto the cleaned silicon wafers at a rate ≤2 Å/s in a diffusion-pumped chamber at a base pressure of 4×10^{-6} Torr. The wafers then were typically cut into 1.2 cm × 4 cm samples after evaporation.

The gold-coated wafers were placed into 1 mM ethanolic solution of 4-mercapto-1-butanol for at least 1 h to yield a hydroxyl-terminated self-assembled monolayer (SAM) on the gold surface. The films were subsequently rinsed with ethanol, water, and ethanol and dried in a stream of nitrogen, followed by exposure to a 5 mM solution of NBDAC in DCM for at least 30 min to yield the acylation product of a surface-tethered norbornenyl group. The norbornenyl-modified substrates were rinsed with DCM, ethanol, water, and ethanol and dried in a stream of nitrogen. Then the substrates were exposed to a 5

DOI: 10.1021/acs.jpcc.9b06410
J. Phys. Chem. C 2019, 123, 23511−23519

Scheme 1. SiROMP of NBDAC and Its Modification with Water, Alcohols, and Amines

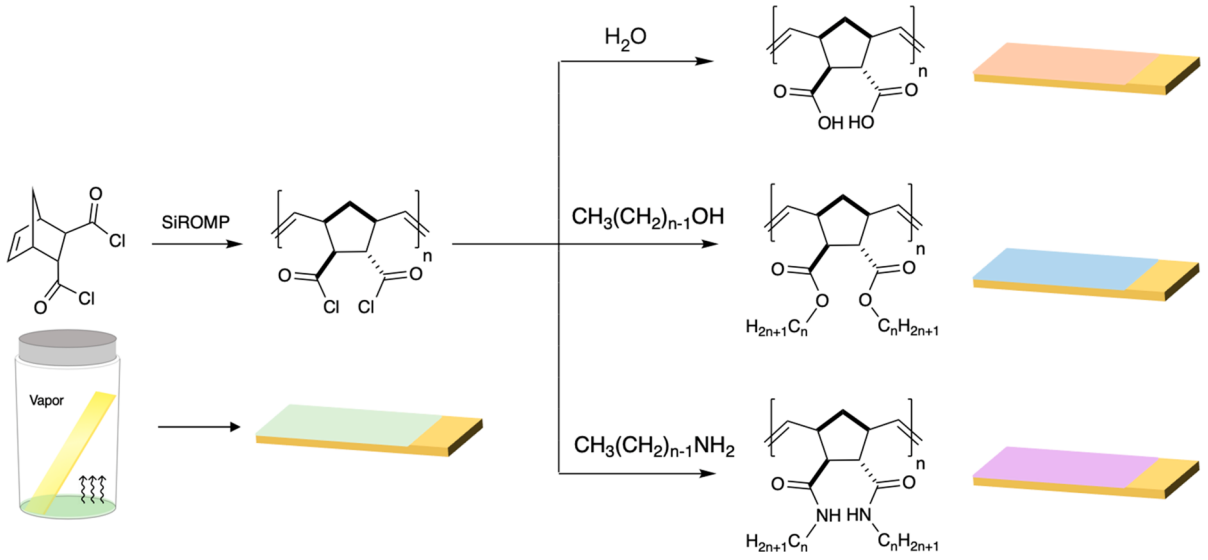

mM solution of Grubbs third generation catalyst ([(H_2IMes)-$(3\text{-}Brpy)_2(Cl)_2Ru{=}CHPh$]) in DCM for 12 min.

Polymerization and Postpolymerization Modification. Polymerization of NBDAC to pNBDAC was accomplished in the vapor phase. The ROMP-active substrates removed from the Grubbs third generation catalyst solution were quickly rinsed with DCM, dried in a stream of nitrogen, and immediately placed into a preheated reaction vial (65 °C) containing pure liquid NBDAC monomer (Scheme 1). NBDAC monomers from the vapor phase were then polymerized onto the catalyst-modified surface to form a smooth thin film. After the surface-initiated polymerization in the vial, the substrates were quickly rinsed with DCM to remove any additional monomer on the film surface and then directly exposed to the reagent for further modification. Water, 2 M ethylamine in THF, ethanol, dimethylethanolamine, or aniline was used to modify pNBDAC films via overnight exposure. An aqueous solution of 0.1 M hydroxylamine was used to modify the pNBDAC films to hydroxamic acid-modified films (HA-modified) via overnight exposure. Metal chelation was accomplished with 30 min exposure of the HA-modified films to 0.03 M concentrations of the transition metal salt solutions.

Characterization Methods. Polarization modulation infrared reflectance−absorption spectroscopy (PM-IRRAS) was performed by using a Bruker Tensor 27 Fourier transform infrared spectrometer equipped with a PEM-90 photoelastic modulator (Hinds Instruments) and a liquid-nitrogen-cooled mercury cadmium telluride (MCT) detector with a non-dichroic BaF_2 window. The source beam employed a half-wavelength ($\lambda/2$) retardation modulated at a frequency of 50 kHz and set at an 85° angle of incidence to the sample surface. Spectra were collected over 5 min (360 scans) at a resolution of 4 cm^{-1}.

Profilometric thickness and roughness were determined by using a Veeco Dektak 150 profiler with a stylus of 12.5 μm radius and 3 mg of force with a 0.28 μm/sample data collection rate. The thickness was estimated by scratching the film surface, scanning 1 mm across the scratch, and plane-fitting the scan results by using the instrument software. The reported values and ranges represent the averages and standard deviations from at least three independently prepared polymer films.

QCM-D was performed in air with a Biolin Scientific Q-Sense E4 interfaced to a computer and an ISMATEC IPC pump. QCM-D measures the frequency shifts and energy dissipation of a quartz crystal sensor in a precise way and allows the calculation of the added mass and viscoelastic properties of materials deposited onto the sensor by applying models related to the change of frequency and dissipation. In a QCM-D measurement, an alternating current (ac) voltage is applied to excite the crystal to oscillation at its fundamental resonant frequency. By periodically connecting and disconnecting the crystal from the ac voltage, we can determine the frequency (f) and dissipation (D) by fitting the decay of the oscillation. The QCM-D measurements were performed at 25 °C. All f and D measurements are collected at a rate of 200 times per second in ultrapure water or 5 mM $FeSO_4$ solution at a flow rate of 100 μL/min. A clean, pretreated quartz crystal was first analyzed by QCM-D with ultrapure (18.2 MΩ·cm) water at a flow rate of 100 μL/min, and the collected measurements were used as the reference baseline for the data analysis.

Electrochemical impedance spectroscopy (EIS) was performed with a Gamry Instruments Reference 600 potentiostat interfaced to a computer. Measurements were conducted in an electrochemical cell to limit the testing area to 1 cm^2 of each sample. The electrochemical cell consisted of an aqueous solution of 0.1 M KCl with a Ag/AgCl/KCl (3 M) reference electrode, a gold-coated silicon substrate coated with the polymer film as the working electrode, and a gold-coated silicon substrate as the counter electrode. A 5 mV ac voltage was applied to perturb the cell. The frequency of the ac voltage was varied from 100 kHz to 0.1 Hz with 10 points per decade.

RESULTS AND DISCUSSION

Kinetics of pNBDAC Film Growth. Exposure of gold substrates modified with Grubbs third-generation catalyst [$(H_2IMes)(3\text{-}Brpy)_2(Cl)_2Ru{=}CHPh$] to solutions of NBDAC in DCM or to neat NBDAC liquid monomer resulted in little growth of polymer from the surface. In fact, film thicknesses of <30 nm were obtained upon exposure of

DOI: 10.1021/acs.jpcc.9b06410
J. Phys. Chem. C 2019, 123, 23511−23519

catalyst-modified surfaces to a 1 M NBDAC solution in DCM if the monomer was not freshly distilled. However, exposure of the same substrates to the vapor of NBDAC rapidly yielded much thicker polymer films (>350 nm) on the surface. As NBDAC is reactive toward water vapor to form carboxylic acids that can poison the Grubbs catalyst, the vapor-phase process effectively distills the monomer from any trace contaminants with lower vapor pressure. The use of freshly distilled monomer from solution enabled similar thicknesses as those obtained by the vapor-phase route.

To investigate the SiROMP of NBDAC in the vapor phase and examine the control over film growth, the kinetics of pNBDAC film growth was examined. Polymer films were grown for different polymerization times ranging from 1 to 10 min, as shown in Figure 1. Because pNBDAC is not stable long

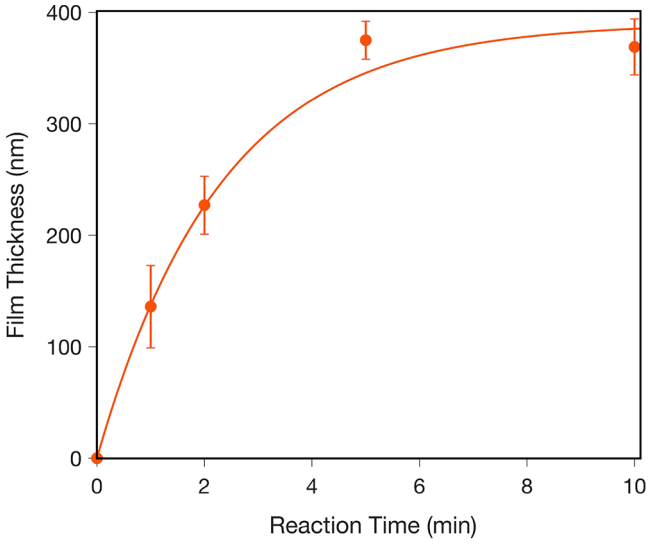

Figure 1. Kinetics plot of pNBDAC film growth via Si-ROMP of NBDAC from the vapor phase at 65 °C. Thicknesses were determined by profilometry. The approximate vapor-phase concentration of NBDAC was 4.4 mM. The data were fit with eq 1 to determine propagation and termination rate constants.

term in ambient air, we modified all the samples with water to produce stable, pendant $-CO_2H$ groups before measuring the thicknesses. The kinetics investigation shows that the rapid polymerization of NBDAC occurs from the vapor phase and that film thickness can be controlled up to 370 nm based on polymerization time under these conditions. To model the data, the film thickness as a function of time can be given as[4,5]

$$d = \left(\frac{KMm_0}{k_t\rho}\right)(1 - e^{-k_t t}) \quad (1)$$

where K is a rate constant that expresses both the initiation and propagation of the polymerization process, M is the concentration of the monomer (4.4 mM from the Clausius–Clapeyron equation),[4] m_0 is the mass of the monomer unit, k_t is the termination rate constant, and ρ is the density of the polymer film (1.35 g/cm^3, estimated to be the same as that of the monomer). The rate constants were calculated as $K = 3.8 \times 10^{-6} \pm 0.3 \times 10^{-6}$ m/s and $k_t = 6.7 \times 10^{-3} \pm 1.2 \times 10^{-3}$ s^{-1} by fitting the experimental data with eq 1. As a comparison, our group has studied the SiROMP of polydicyclopentadiene from the vapor phase in previous work,[4] which has a much faster propagation rate constant with K of $1.5 \times 10^{-4} \pm 0.5 \times 10^{-4}$ m/s but also a faster termination rate constant with k_t of 0.04 ± 0.01 s^{-1}. The slower propagation rate for pNBDAC could be related to interference by the polar groups of the NBDAC monomer with the catalyst, and the slower termination rate is attributed to the reduced content of olefins, which can provide sites for catalyst termination, within pNBDAC versus polydicyclopentadiene.

Post-polymerization Modification of pNBDAC Films. PM-IRRAS was used to confirm the successful preparation of the pNBDAC films on the surface and identify the functional groups in the film after modification (Figure 2). The spectrum

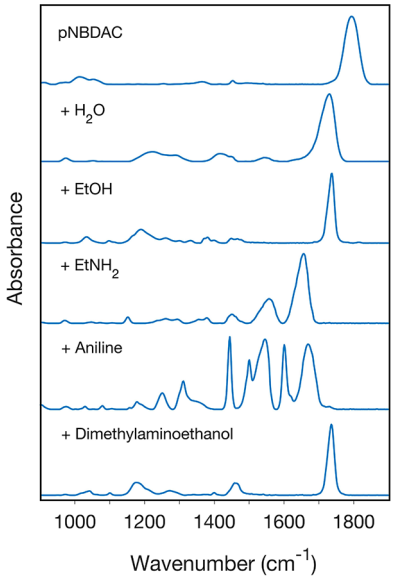

Figure 2. FTIR spectra of pNBDAC and polymer films obtained by modifying pNBDAC with water, ethanol, and ethylamine to create pendant −COOH, −COOEt, and −CONHEt functionality within the film. FTIR spectra of pNBDAC films after exposure to aniline and dimethylethanolamine demonstrate that larger and more diverse molecular groups can be introduced as pendant side chains by this approach.

of the pNBDAC films shows absorption bands due to C═O stretching of the acyl chloride (1794 cm^{-1}), C_{sp^3}–H in-plane bending (1430–1500 cm^{-1}), C_{sp^3}–H out-of-plane bending (1300–1400 cm^{-1}), and C_{sp^2}–H out-of-plane bending (900–1100 cm^{-1}). The spectrum indicates the successful SiROMP of NBDAC from the vapor phase.

Although pNBDAC is too unstable to be utilized as a polymer film long term, it is a very effective intermediate to produce stable polymer films due to the fast and versatile reactions between pendant acyl chlorides and other reagents to create an enormous variety of side-chain compositions. Therefore, as a proof of concept, we investigated the feasibility of modifying pNBDAC films to obtain films with pendant carboxylic acids (−COOH), ethyl esters (−COOEt,) and ethyl amides (−CONHEt) by reacting the polymer film with water, ethanol, and ethylamine, respectively (Scheme 1). The IR spectra of polymer films containing pendant $-CO_2H$, $-CO_2Et$, and −CONHEt side groups are shown in Figure 1, together with the IR spectrum of pNBDAC. The spectrum of the CO_2H-modified film shows absorption bands due to the stretching of C═O (1726 cm^{-1}) and C–O (1200–1350 cm^{-1}) in carboxylic acids. The spectrum of the EtO_2C-

DOI: 10.1021/acs.jpcc.9b06410
J. Phys. Chem. C 2019, 123, 23511–23519

modified film shows absorption bands due to the stretching of C═O (1738 cm^{-1}) and C−O (1130−1300 cm^{-1}) of esters. The spectrum of the −CONHEt modified film shows absorption bands due to C═O stretching (1657 cm^{-1}) and N−H bending (1557 cm^{-1}) in amides. Importantly, these spectra also show the complete diminution of the C═O stretching at 1794 cm^{-1} due to the acyl chloride functionality to signal complete modification of the original pNBDAC film with these three different pendant functional groups. These results confirm the feasibility of utilizing pNBDAC films as an intermediate to prepare other functional polymers. By extending the modification agent to any type of alcohol, amine, or any other molecule with functional groups that react with acyl chlorides, this pNBDAC base film would enable the preparation of an unlimited array of surface-attached polymer films.

We also examined the modification of pNBDAC with molecular reagents beyond simple alcohols and amines to confirm the versatility of the modification method. The grown pNBDAC films were exposed overnight to aniline or 2-dimethyl-aminoethanol, and PM-IRRAS measurements were taken after the modification process. The modification of the pNBDAC film with aniline demonstrates that aromatic groups can also be introduced quantitatively into the film. The IR spectrum of the formed anilide shows absorption bands due to C═O stretching (1668 cm^{-1}), aromatic C═C ring stretching (1500−1610 cm^{-1}), and C−N stretching (1250 and 1310 cm^{-1}). Quantitative modification of pNBDAC with 2-dimethylaminoethanol is supported by the complete diminution of the C═O stretching band at 1794 cm^{-1} and new absorption bands due to C═O stretching of the ester (1736 cm^{-1}) and C−N stretching (1270 cm^{-1}). These various modifications indicate that the method is tolerant of more diverse functional groups than those imparted by unsubstituted n-alcohols or n-amines.

Figure 2 shows that pNBDAC can be reacted with alcohols to form esters and amines to form amides. On the basis of the greater nucleophilicity of the amine, we would expect the amines to react more favorably with the acyl chlorides than alcohols do. Hydroxylamine, containing both an amine and an alcohol, serves as a valid test molecule to determine the selectivity of the reaction with the acyl chlorides in pNBDAC. If the amine reacts with the acyl chlorides to form an amide, then the resulting group will be a hydroxamic acid.

Preparation of Hydroxamic Acid-Modified Films. Exposure of pNBDAC films with thicknesses of ∼300 nm overnight in a 0.1 M hydroxylamine aqueous solution results in modification of the acyl chloride groups to hydroxamic acids. Compared to the IR spectrum of pNBDAC in Figure 3, the spectrum of the film after exposure to hydroxylamine shows complete diminution of the C═O stretching due to the acyl chloride at 1794 cm^{-1} and the appearance of strong absorption bands due to C═O stretching (1666 cm^{-1}) of the amide and N−O stretching (1500−1550 cm^{-1}) in hydroxamic acid, which demonstrates the successful film modification. In addition, a weak absorption band due to C═O stretching in ester (1739 cm^{-1}) is also observed. The much stronger absorbance due to amide versus ester indicates that the modification process with hydroxylamine is far more selective to form amide rather than ester side chains, which is noteworthy considering that both alcohols and amines react readily with the pendant acyl chlorides (Figure 2).

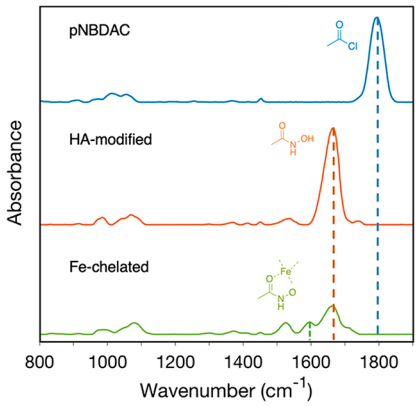

Figure 3. IR spectra of the original pNBDAC film and the hydroxamic acid-modified film (HA-modified) before and after exposure to a Fe^{2+} salt to yield the Fe-chelated film.

Chelation of Transition Metal Ions with the HA-Modified Films. The chelation ability of the prepared HA-modified films was tested with the divalent ion Fe^{2+}. The obtained HA-modified film was exposed to 0.03 M $FeSO_4$ aqueous solution for 30 min, and the IR spectrum of the resulting film is shown in Figure 3. Two significant changes in the IR spectrum of the Fe^{2+} chelated film as compared to that of the original HA-modified film are the dramatically reduced intensity of the absorption band due to C═O stretching in hydroxamic acid (1666 cm^{-1}) and the appearance of an absorption band at 1597 cm^{-1} due to C═O stretching in the chelated structure, which signals the existence of the Fe^{2+}-HA chelation in the resulting film.[40] However, the IR spectrum also shows that not all the hydroxamic acid groups in the film are chelated with the Fe^{2+}. The incomplete conversion is consistent with previous literature on chelation. Considering that two center-symmetric hydroxamic acid groups are required to chelate Fe^{2+},[30] not all the hydroxamic acid groups would be positioned or oriented to form such a center-symmetric structure, and thus, a portion of unchelated hydroxamic acid groups are left after the exposure to iron(II) salt solution. By deconvolution of these IR peaks (shown in Figure S3 of the Supporting Information) and assuming that integrated peak intensity scales with concentration of groups within the film, we estimate that 69% of the hydroxamic acids form a chelated complex with Fe. This level of complexation would provide an Fe concentration of ∼3 M within the polymer film. Other noticeable changes are the disappearance of the absorption band due to C═O stretching (1739 cm^{-1}) and newly formed absorption band at 1710 cm^{-1} due to C═O stretching in carboxylic acid. The C═O stretching shifting from 1739 to 1710 cm^{-1} is due to the hydrolysis of the residual esters, in good agreement with the use of divalent metal ions as catalysts for the hydrolysis of esters with amino groups.[43,44]

The chelation ability of the prepared HA-modified films with several other transition metal ions beyond Fe^{2+} was also tested and compared. The HA-modified films were exposed overnight separately to 0.03 M solutions of Cu^{2+}, Co^{2+}, and Zn^{2+}. The IR spectra of the HA-modified films before and after exposure to metal ion solutions are shown in Figure 4. All IR spectra show significant decrease of the carbonyl intensity for the hydroxamic acid group after exposure to the metal ion solutions, indicating successful chelation of divalent metal ions. From Figure 4, the percentages of chelation relative to the

DOI: 10.1021/acs.jpcc.9b06410
J. Phys. Chem. C 2019, 123, 23511−23519

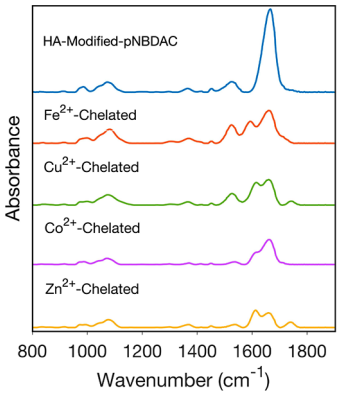

Figure 4. IR spectra of HA-modified pNBDAC films before and after chelation of various divalent metal ions.

hydroxamic acid content are 69% (Fe), 63% (Cu), 56% (Co), and 76% (Zn).

Effect of Fe Chelation on Film Properties. The chelation of metals plays an important role in altering the properties of these polymer films. Two center-symmetric hydroxamic acids are required to chelate a ferrous ion, which means that the metal chelation does not occur within the monomer unit of these films but occurs between different units or even across different polymer chains. In this case, chelated metal ions also function as cross-linkers, changing the structure and properties of the film.

Stability is important for surface-initiated polymer thin films as they are investigated for many different applications. The prepared HA-modified pNBDAC films show stability in air and in water at room temperature. However, the film can be easily detached from the gold surface when placed in water at 80 °C (Figure 5). The decrease in stability is mainly due to the stronger interaction of the polymer chain with the aqueous environment. At the high temperature, the polymer chains have sufficient energy of motion to overcome the thiol−Au bond that affixes the film to the substrate. At high pH, the

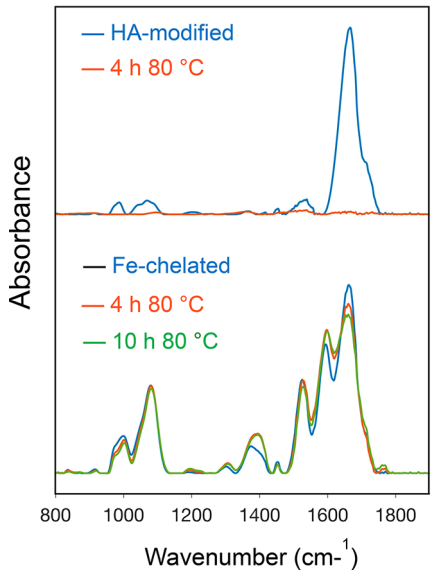

Figure 5. IR spectra of an HA-modified pNBDAC film and an Fe-chelated film, both before and after exposure to 80 °C water for the indicated times.

hydroxamic acid groups will become deprotonated to hydroxamates,[40] which significantly increases the interaction of the film with water. In both cases, the chelated metal ions can behave as cross-linkers, which would make the structure less swellable in solution and increase the film stability. Film stability investigations were performed for both the HA-modified film and the Fe^{2+} chelated film.

To investigate the film stability in solution at high temperature, the HA-modified film and Fe^{2+} chelated film were placed in 80 °C deionized water for 4 h. The HA-modified film was quickly removed from the surface while the chelated film was stable on the surface. The chelated film was then placed back in the 80 °C deionized water for an additional 6 h to examine the longer term stability. The IR spectra in Figure 5 show that the film is still stable after soaking in 80 °C water for 10 h. We also tested the stability of the films with different chelation percentages. Table 1 demonstrates that even

Table 1. Thermal Stability of the Film with Different Chelation Percentages upon Exposure to 80 °C Water for 10 h

chelation percentage (%)	stability?
0	unstable
27	stable
60	stable
69	stable

a low percentage of partial chelation (e.g., 27%) is enough to stabilize the films in a cross-linked structure that reduces chain motion and is less swellable in solution to enhance the thermal stability of the film. The Fe-chelated films are stable not only to high temperatures but also to a broad range of pH, spanning from 1 to 13 (see Figures S1 and S2).

The effect of Fe chelation on the interaction of the film with water can be characterized by employing QCM-D. QCM-D is a technique that provides precise measurements of resonant frequency shifts and energy dissipation factor of a QCM crystal upon loading with a film or coating. The addition of film mass on the quartz crystal will result in a decrease in the frequency of oscillations, while varying the viscoelastic properties of the film can be related to the energy dissipation of the coated crystal. The interaction of the polymer film with water can be directly demonstrated by the change in energy dissipation, with the mechanical properties indicating the phase state of the film in the solution. We collected the frequency and dissipation values for a clean quartz crystal sensor with flowing water and used those as the baseline. The changes in frequency (Δf) and energy dissipation (ΔD) as we deposited the HA-modified pNBDAC film and chelated Fe^{2+} into the film on the crystal are shown in Figure 6. Both the addition of the HA-modified film on the crystal and the chelation of Fe^{2+} into the film result in a decrease in frequency, which shows that masses have been deposited onto the crystal. A mass ratio of the chelated Fe^{2+} to the original HA-modified film (0.15) is obtained by applying the Kelvin−Voigt model. Then, on the basis of molecular weights of Fe^{2+} and the repeating unit, we estimated that 74% percent of the hydroxamic acid groups have been chelated with Fe^{2+}. The chelation degree is similar to that of 69% evaluated based on the IR spectra.

QCM can also be used to evaluate the viscoelastic properties of the coated crystal in the aqueous solution by analyzing the change in dissipation (ΔD). In the Kelvin−Voigt model, a

DOI: 10.1021/acs.jpcc.9b06410
J. Phys. Chem. C 2019, 123, 23511−23519

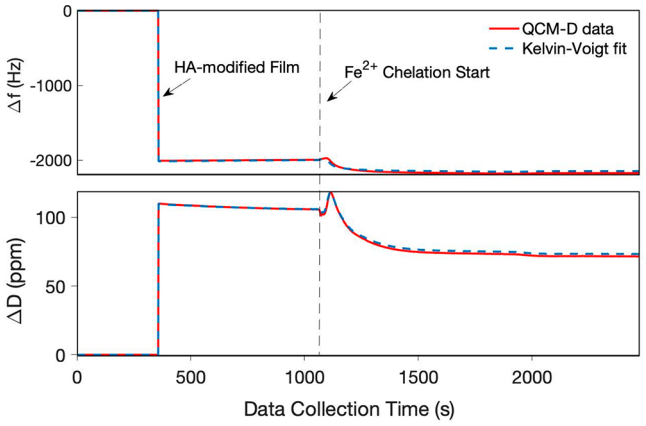

Figure 6. QCM analysis of the bare crystal and the HA-modified film (grown ex situ on the QCM crystal) before and after exposure to 0.03 mM Fe^{2+}(aq) to achieve the Fe-chelated film.

complex shear modulus is used to present the viscoelastic properties of the film

$$G = G' + jG'' \quad (2)$$

where G' is the shear storage modulus that describes the solid behavior of the material, and G'' is the shear loss modulus that describes the liquid behavior of the material. In our experiments, after the chelation of Fe^{2+}, the shear storage modulus increased by 65% and the shear loss modulus decreased by 47%, which shows that the existence of chelated Fe^{2+} results in a more solid-like and less liquid-like behavior of the material in the aqueous solution. Therefore, the changes in complex shear moduli are consistent with Fe-chelated cross-linking in the polymer film.

Effect of Fe Chelation on Ion Transport in the Chelated Film. Ion transport through the HA-modified and Fe-chelated films was investigated with EIS by using a gold substrate with the film attached as the working electrode. The frequency response of the system was recorded by applying a frequency-varied ac potential of 5 mV and plotted in the format of a Bode magnitude plot (Figure 7). In the Bode plots, the EIS spectra of HA-modified film and the norbornene-tethered SAM have similar shape, which demonstrates that the additional polymer film attached on the SAM-modified substrate does not provide significant resistance against the ion transport from the solution to the surface. The result agrees with that from QCM-D to show that HA-modified films are swollen in the aqueous solution. For the EIS spectrum of the Fe-chelated film, there is substantial change in the frequency range of 100−20000 Hz. The near plateau shown in the spectrum represents the resistance that the chelated film provides against ion transfer, which results from the cross-linked and less swellable structure upon chelation of Fe^{2+}. This resistance of $(1.4 \pm 0.1) \times 10^3$ Ω·cm^2 for the Fe-chelated film is at least 15 times greater than any resistance provided by the HA-modified film, which is so low here that it cannot be distinguished from the solution resistance.

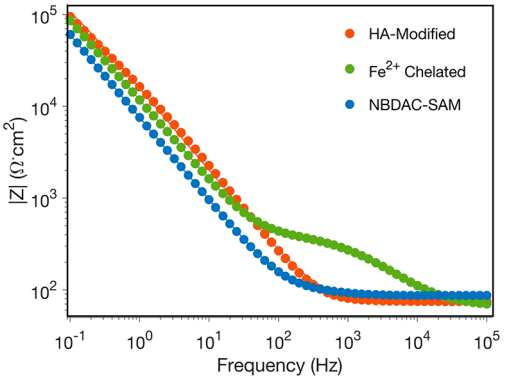

Figure 7. Electrochemical impedance spectra in the form of Bode magnitude plots of the HA-modifed pNBDAC and Fe^{2+} chelated films, with the spectrum of NBDAC-modified SAM as a control. Fits of the spectra are provided by an equivalent circuit model for a polymer thin film reported previously.[18]

CONCLUSIONS

PNBDAC films were successfully prepared via SiROMP of NBDAC from the vapor phase. This method ensures rapid kinetics of film growth with film thicknesses reaching more than 350 nm. By exposure of pNBDAC films to compounds such as water, alcohols, and amines, the chains can be easily modified to produce films with various pendant functionalities with high conversion. Thus, pNBDAC provides an excellent scaffold to build many different types of polymer films. Exposure of pNBDAC to hydroxylamine results in a high conversion of the acyl chlorides to hydroxamic acids. These hydroxamic acids can chelate various divalent metal ions, including iron, cobalt, copper, and zinc, with high loadings. The presence of the metals cross-links the polymer chains to greatly alter film properties. The stability of the film in 80 °C water is dramatically improved by the chelation of Fe, even at levels as low as 27%. Chelation of Fe at higher levels (∼70%) produces a film with higher shear storage modulus and reduced shear loss modulus, consistent with a more solid-like film with greater cross-linking, than the original film before modification with Fe. The chelation also boosts the resistance of the film to aqueous ion transfer over that of the original film. The enhanced stability of these metal chelated films suggest that they could be utilized in many applications where thin films are exposed to harsh environments.

ASSOCIATED CONTENT

Supporting Information

The Supporting Information is available free of charge on the ACS Publications website at DOI: 10.1021/acs.jpcc.9b06410.

Investigation of the stability of the metal-chelated film in various pH environments; discussion of the peak deconvolution method of the HA-modified films and metal-chelated films (PDF)

AUTHOR INFORMATION

Corresponding Author

*E-mail: kane.g.jennings@vanderbilt.edu. Phone: 615 322 2707.

ORCID

G. Kane Jennings: 0000-0002-3531-7388

Notes

The authors declare no competing financial interest.

ACKNOWLEDGMENTS

We gratefully acknowledge the financial support of the Department of Energy through Grant DE-NE0008712. The

DOI: 10.1021/acs.jpcc.9b06410
J. Phys. Chem. C 2019, 123, 23511−23519

authors thank the staff at the Vanderbilt Institute of Nanoscale Science and Engineering (VINSE) for their support.

REFERENCES

(1) Olivier, A.; Meyer, F.; Raquez, J. M.; Damman, P.; Dubois, P. Surface-Initiated Controlled Polymerization as a Convenient Method for Designing Functional Polymer Brushes: From Self-Assembled Monolayers to Patterned Surfaces. *Prog. Polym. Sci.* **2012**, *37* (1), 157−181.
(2) Edmondson, S.; Osborne, V. L. V.; Huck, W. T. S. Polymer Brushes via Surface-Initiated Polymerizations. *Chem. Soc. Rev.* **2004**, *33* (1), 14−22.
(3) Faulkner, C. J.; Fischer, R. E.; Jennings, G. K. Surface-Initiated Polymerization of 5-(Perfluoro-n-Alkyl)Norbornenes from Gold Substrates. *Macromolecules* **2010**, *43* (3), 1203−1209.
(4) Njoroge, I.; Kempler, P.; Deng, X.; Arnold, S.; Jennings, G. K. Surface-Initiated Ring-Opening Metathesis Polymerization of Dicyclopentadiene from the Vapor Phase. *Langmuir* **2017**, *33*, 13903.
(5) Escobar, C. A.; Harl, R. R.; Maxwell, K. E.; Mahfuz, N. N.; Rogers, B. R.; Jennings, G. K. Amplification of Surface-Initiated Ring-Opening Metathesis Polymerization of 5-(Perfluoro-n-alkyl)-Norbornenes by Macroinitiation. *Langmuir* **2013**, *29*, 12560−12571.
(6) Buchmeiser, M. R.; Sinner, F.; Mupa, M.; Wurst, K. Ring-Opening Metathesis Polymerization for the Preparation of Surface-Grafted Polymer Supports. *Macromolecules* **2000**, *33* (1), 32−39.
(7) Lerum, M. F. Z.; Chen, W. Surface-Initiated Ring-Opening Metathesis Polymerization in the Vapor Phase: An Efficient Method for Grafting Cyclic Olefins with Low Strain Energies. *Langmuir* **2011**, *27* (9), 5403−5409.
(8) Minet, I.; Delhalle, J.; Hevesi, L.; Mekhalif, Z. Surface-Initiated ATRP of PMMA, PS and Diblock PS-b-PMMA Copolymers from Stainless Steel Modified by 11-(2-Bromoisobutyrate)-Undecyl-1-Phosphonic Acid. *J. Colloid Interface Sci.* **2009**, *332* (2), 317−326.
(9) Bissadi, G.; Weberskirch, R. Formation of Polyoxazoline-Silica Nanoparticles: Via the Surface-Initiated Cationic Polymerization of 2-Methyl-2-Oxazoline. *Polym. Chem.* **2016**, *7* (32), 5157−5168.
(10) Min, J.; Lin, Y.; Zheng, J.; Tang, T. A Novel Strategy to Synthesize Well-Defined PS Brushes on Silica Particles by Combination of Lithium-Iodine Exchange (LIE) and Surface-Initiated Living Anionic Polymerization (SI-LAP). *Chem. Commun.* **2015**, *51* (27), 5921−5924.
(11) Balachandra, A. M.; Baker, G. L.; Bruening, M. L. Preparation of Composite Membranes by Atom Transfer Radical Polymerization Initiated from a Porous Support. *J. Membr. Sci.* **2003**, *227*, 1−14.
(12) Ulbricht, M. Advanced Functional Polymer Membranes. *Polymer* **2006**, *47* (7), 2217−2262.
(13) Leitgeb, A.; Wappel, J.; Slugovc, C. The ROMP Toolbox Upgraded. *Polymer* **2010**, *51* (14), 2927−2946.
(14) Bielawski, C. W.; Grubbs, R. H. Living Ring-Opening Metathesis Polymerization. *Prog. Polym. Sci.* **2007**, *32* (1), 1−29.
(15) Sutthasupa, S.; Shiotsuki, M.; Sanda, F. Recent Advances in Ring-Opening Metathesis Polymerization, and Application to Synthesis of Functional Materials. *Polym. J.* **2010**, *42* (12), 905−915.
(16) Montembault, V.; Desbrosses, J.; Campistron, I.; Reyx, D. Ring-Opening Metathesis Polymerization of 2-(S)-(−)-Endo-D-Pantolacton-O-yl Norbornene-2-Carboxylate Using a Classical ROMP Catalyst. Synthesis and Characterization of Optically Active Poly-(Norbornene-2-Carboxylic Acid). *Macromol. Chem. Phys.* **2000**, *201* (9), 973−979.
(17) Buchmeiser, M. R.; Atzl, N.; Bonn, G. K. Ring-Opening-Metathesis Polymerization for the Preparation of Carboxylic-Acid Functionalized, High-Capacity Polymers for Use in Separation Techniques. *J. Am. Chem. Soc.* **1997**, *119* (39), 9166−9174.
(18) Njoroge, I.; Matson, M. W.; Jennings, G. K. Dynamic Anion-Adaptive Poly(Ionic Liquid) Films via Surface-Initiated Ring-Opening Metathesis Polymerization. *J. Phys. Chem. C* **2017**, *121* (37), 20323−20334.
(19) Morrison, R. T.; Boyd, R. N. *Organic Chemistry*; Prentice Hall: 1992.
(20) Yang, Y. S.; Qi, G. R.; Qian, J. W.; Yang, S. L. Acryloyl Chloride Polymer. *J. Appl. Polym. Sci.* **1998**, *68* (April), 665−670.
(21) Buruiana, E. C.; Buruiana, T.; Hahui, L. Preparation and Characterization of New Optically Active Poly (N -Acryloyl Chloride) Functionalized with (S)-Phenylalanine and Pendant Pyrene. *J. Photochem. Photobiol., A* **2007**, *189*, 65−72.
(22) Wang, X.; Zhang, C.; Du, Z.; Li, H.; Zou, W. Synthesis of Non-Destructive Amido Group Functionalized Multi-Walled Carbon Nanotubes and Their Application in Antistatic and Thermal Conductive Polyetherimide Matrix Nanocomposites. *Polym. Adv. Technol.* **2017**, *28*, 791−796.
(23) Moore, J. D.; Byrne, R. J.; Vedantham, P.; Flynn, D. L.; Hanson, P. R. High-Load, ROMP-Generated Oligomeric Bis-Acid Chlorides: Design of Soluble and Insoluble Nucleophile Scavengers. *Org. Lett.* **2003**, *5* (23), 4241−4244.
(24) Rolfe, A.; Loh, J. K.; Maity, P. K.; Hanson, P. R. High-Load, Hybrid Si-ROMP Reagents. *Org. Lett.* **2011**, *13* (1), 4−7.
(25) Fu, D.; Weng, L. T.; Du, B.; Tsui, O. K. C.; Xu, B. Solventless Polymerization at the Gas-Solid Interface to Form Polymeric Thin Films. *Adv. Mater.* **2002**, *14* (5), 339−343.
(26) Feng, J.; Stoddart, S. S.; Weerakoon, K. A.; Chen, W. An Efficient Approach to Surface-Initiated Ring-Opening Metathesis Polymerization of Cyclooctadiene. *Langmuir* **2007**, *23* (3), 1004−1006.
(27) Tian, F.; Roman, M. J.; Decker, E. A.; Goddard, J. M. Biomimetic Design of Chelating Interfaces. *J. Appl. Polym. Sci.* **2015**, *132*, 2−9.
(28) Duran, A.; Soylak, M.; Tuncel, S. A. Poly(Vinyl Pyridine-Poly Ethylene Glycol Methacrylate-Ethylene Glycol Dimethacrylate) Beads for Heavy Metal Removal. *J. Hazard. Mater.* **2008**, *155*, 114−120.
(29) Zhang, Z.; Li, J.; Song, X.; Ma, J.; Chen, L. Hg^{2+} Ion-Imprinted Polymers Sorbents Based on Dithizone−Hg2+ Chelation for Mercury Speciation Analysis in Environmental and Biological Samples. *RSC Adv.* **2014**, *4*, 46444−46453.
(30) Rahman, M. L.; Sarkar, S. M.; Yusoff, M. M.; Abdullah, M. H. Optical Detection and Efficient Removal of Transition Metal Ions from Water Using Poly(Hydroxamic Acid) Ligand. *Sens. Actuators, B* **2017**, *242*, 595−608.
(31) Rahman, M. L.; Biswas, T. K.; Sarkar, S. M.; Yusoff, M. M.; Sarjadi, M. S.; Arshad, S. E.; Musta, B. Adsorption of Rare Earth Metals from Water Using a Kenaf Cellulose-Based Poly (Hydroxamic Acid) Ligand. *J. Mol. Liq.* **2017**, *243*, 616−623.
(32) Liu, Z.; Lin, T.; Purro, M.; Xiong, M. P. Enzymatically Biodegradable Polyrotaxane-Deferoxamine Conjugates for Iron Chelation. *ACS Appl. Mater. Interfaces* **2016**, *8* (39), 25788−25797.
(33) Qian, J.; Sullivan, B. P.; Peterson, S. J.; Berkland, C. Nonabsorbable Iron Binding Polymers Prevent Dietary Iron Absorption for the Treatment of Iron Overload. *ACS Macro Lett.* **2017**, *6*, 350−353.
(34) Liu, Z.; Purro, M.; Qiao, J.; Xiong, M. P. Multifunctional Polymeric Micelles for Combining Chelation and Detection of Iron in Living Cells. *Adv. Healthcare Mater.* **2017**, DOI: 10.1002/adhm.201770087.
(35) Choudhury, S.; Connolly, D.; White, B. Supermacroporous PolyHIPE and Cryogel Monolithic Materials as Stationary Phases in Separation Science: A Review. *Anal. Methods* **2015**, *7* (17), 6967−6982.
(36) Moyna, Á.; Connolly, D.; Nesterenko, E.; Nesterenko, P. N.; Paull, B. Separation of Selected Transition Metals by Capillary Chelation Ion Chromatography Using Acetyl-Iminodiacetic Acid Modified Capillary Polymer Monoliths. *J. Chromatogr. A* **2012**, *1249*, 155−163.
(37) Winston, A.; Mazza, E. T.; Virginia, W. Hydroxamic Acid Polymers. *J. Polym. Sci., Polym. Chem. Ed.* **1975**, *13*, 2019−2030.
(38) Winston, A.; McLaughlin, G. R.; Virginia, W. Hydroxamic Acid Polymers. II. Design of a Polymeric Chelating Agent for Iron. *J. Polym. Sci., Polym. Chem. Ed.* **1976**, *14*, 2155−2165.
(39) Kumar, S. A.; Pandey, S. P.; Shenoy, N. S.; Kumar, S. D. Matrix Separation and Preconcentration of Rare Earth Elements from

DOI: 10.1021/acs.jpcc.9b06410
J. Phys. Chem. C 2019, 123, 23511−23519

Seawater by Poly Hydroxamic Acid Cartridge Followed by Determination Using ICP-MS. *Desalination* **2011**, *281*, 49−54.
(40) Roman, M. J.; Decker, E. A.; Goddard, J. M. Fourier Transform Infrared Studies on the Dissociation Behavior of Metal-Chelating Polyelectrolyte Brushes. *ACS Appl. Mater. Interfaces* **2014**, *6*, 5383−5387.
(41) Agrawal, Y. K.; Kaur, H.; Menon, S. K. Poly (Styrene-p-Hydroxamic Acids): Synthesis, and Ion Exchange Separation of Rare Earths. *React. Funct. Polym.* **1999**, *39*, 155−164.
(42) Love, J. A.; Sanford, M. S.; Day, M. W.; Grubbs, R. H. Synthesis, Structure, and Activity of Enhanced Initiators for Olefin Metathesis. *J. Am. Chem. Soc.* **2003**, *125* (33), 10103−10109.
(43) Sutton, P. A.; Buckingham, D. A. Cobalt (III) -Promoted Hydrolysis of Amino Acid Esters and Peptides and the Synthesis of Small Peptides. *Acc. Chem. Res.* **1987**, *20* (10), 357−364.
(44) Fife, T. H.; Przystas, T. J. Divalent Metal Ion Catalysis in the Hydrolysis of Esters of Picolinic Acid. Metal Ion Promoted Hydroxide Ion and Water Catalyzed Reactions. *J. Am. Chem. Soc.* **1985**, *107* (14), 1041−1047.

DOI: 10.1021/acs.jpcc.9b06410
J. Phys. Chem. C 2019, 123, 23511−23519